Comparison of the Lamellar Morphology of Microphase-Separated Cyclic Block Copolymers and Their Linear Precursors

R. L. Lescanec,[†,‡] D. A. Hajduk,[§] G. Y. Kim,[†] Y. Gan,[∥] R. Yin,[∥] S. M. Gruner,[§] T. E. Hogen-Esch,[∥] and E. L. Thomas*[,†]

Department of Materials Science and Engineering, Massachusetts Institute of Technology, Cambridge, Massachusetts 02139, Department of Physics, Princeton University, Princeton, New Jersey 08544, and Loker Hydrocarbon Research Institute and Department of Chemistry, University of Southern California, University Park, Los Angeles, California 90089

Received December 6, 1994

In this paper, we examine a new block copolymer architecture—cyclic block copolymers. The physical behavior of cyclic polymers, both in solution[1] and in the bulk,[2,3] has been the subject of continual research. Current issues concern their dynamics[4,5] and topological characteristics.[6–9] Due to the challenges present in the synthesis of cyclic polymers,[10] the morphology of microphase-separated cyclic block copolymer systems has not been investigated previously. Recently, however, well-characterized cyclic polystyrene–poly(2-vinylpyridine) (PS–P2VP) and polystyrene–poly(dimethylsiloxane) (PS–PDMS) block copolymers have been synthesized from their linear triblock precursors.[11–13] The morphology of these microphase-separated systems is the topic of the present study.

The focus of our study is to probe the effect of loops versus bridges on the morphological characteristics of microphase-separated block copolymer systems. Cyclic A–B diblocks only assume doubly-looped chain conformations in the microphase-separated state, while their linear A–B–A triblock precursors are looped and bridged. We anticipate this difference to be manifest in the relative spacings of their respective microlattices. The microstructural characteristics of these systems are examined through transmission electron microscopy (TEM) and small-angle X-ray scattering (SAXS) of systems exhibiting varying degrees of quench into the microphase-separated state. These observations are then compared to our theoretical predictions.

Cyclic PS–P2VP and PS–PDMS were prepared by end-coupling their linear triblock precursors bis-anionic LiP2VP–PS–P2VPLi and LiPDMS–PS–PDMSLi with 1,4-bis(bromomethyl)benzene and $Cl_2Si(CH_3)_2$, respectively. The details of the synthesis of the precursor triblocks, coupling reactions, and characterization of the block copolymers are given elsewhere.[11–13] The molecular characteristics of the cyclic diblock and linear triblock precursors used in this study are shown in Table 1. The nomenclature used to describe the samples is as follows: $(PDMS–PS–PDMS)_l$ 6/15/6 is a linear PDMS–PS–PDMS triblock copolymer, where M_w = 6450 for each the two PDMS outer blocks and M_w = 14 800 for the polystyrene middle block. The cyclic systems are named in a similar fashion.

Specimens for TEM and SAXS characterization were quiescently cast from a toluene solution (~5% w/v) over a period of 1 week. Toluene was selected as the solvent since it is a good compromise to a nonpreferential solvent for these systems.[14] The resulting films, approximately 1 mm thick, were then placed under vacuum at room temperature for 1 day to remove any residual solvent. In an effort to obtain near-equilibrium microstructures, the films were subsequently annealed above the T_g of the PS and P2VP components, at 115 °C for 5 days, under vacuum. We expect these conditions will yield microstructures with optimum long-range order.[15]

Ultrathin sections (~50 nm) for TEM characterization were obtained by microtomy at ambient conditions using a Reichert-Jung FC4E microtome equipped with a diamond knife. To enhance mass–thickness contrast in the PS–P2VP systems, the microtomed sections were stained with CH_3I vapors. The domains in the PS–PDMS systems have sufficient electron density differences to enable TEM observation of unstained sections. Bright-field TEM was performed on a JEOL-200CX transmission electron microscope equipped with a tungsten filament operated at an accelerating voltage of 100 kV.

SAXS was performed using Cu Kα X-rays from a Rigaku RU-200BH rotating-anode X-ray generator equipped with a 0.2 × 2 mm microfocus cathode and Franks mirror optics. Two-dimensional images were collected with an image-intensified area CCD detector.[16] After collection, the images were digitized and corrected for detector response characteristics. Domain spacings were calculated from one-dimensional intensity profiles obtained by integrating the two-dimensional patterns azimuthally along an arc ±15° from the axis normal to the polymer film surface. Obtaining domain spacings by this method is preferable to measuring the periodicity of the bright-field images due to the possible effect of microdomain swelling from the use of stain. Also, the microdomains are viewed in projection, and the grains are often tilted. This may also lead to inaccurate domain spacing measurements. Accurate measurements are critical in our case since we will be discriminating between small differences in the domain spacings of structures formed by the cyclic and linear systems.

The thermodynamics of our systems are addressed through density functional theory.[17,18] The grand potential form of our free energy is a function of both the total system density profile, $\varrho(\mathbf{r})$, and the minority-component density profile in the microphase-separated state, $\varrho_A(\mathbf{r})$, that is, $\Omega = \Omega[\varrho(\mathbf{r}),\varrho_A(\mathbf{r})]$. The free energy description assumes that the block copolymers are noncrystallizable, monodisperse, and that both blocks have equal statistical segment lengths and volumes. In evaluating the free energy, we will consider all chains to be Gaussian in the disordered state and ignore any effects that result from the topological characteristics (i.e., knottedness) present in cyclic systems. We will further assume that our systems are incompressible, such that $\varrho(\mathbf{r}) = \varrho$, the total density of the homogeneous state. Therefore, $\Omega = \Omega[\varrho_A(\mathbf{r})] = F[\varrho_A(\mathbf{r})]$, where F is the Helmholtz free energy in the microphase-separated state.

We write $F[\varrho_A(\mathbf{r})]$ as a functional Taylor series expansion about its value in the homogeneous phase, which is described as a Landau expansion[19] in the density variable $\varrho_A(\mathbf{r})$, with the vertex function Γ_i as the coefficient of the ith term in the expansion. These

[†] Massachusetts Institute of Technology.
[‡] Present address: Department of Polymer Science, University of Southern Mississippi, Hattiesburg, MS 39406.
[§] Princeton University.
[∥] University of Southern California.

0024-9297/95/2228-3485$09.00/0 © 1995 American Chemical Society

Table 1. Characteristics of the Cyclic and Linear Block Copolymers and Their Lamellar Microphases

sample	M_w[a]	M_w/M_n[a]	f_{PS}[b]	N	χN	D (Å)[c]	D_c/D_l[d]
$(PS-PDMS)_c$ 15/12	14 800–12 900	1.29	0.53	296	89	129	0.95 (0.96)
$(PDMS-PS-PDMS)_l$ 6/15/6	6450–14 800–6450	1.24	0.53	296	89	136	0.95 (0.96)
$(PS-PDMS)_c$ 36/38	35 800–37 200	1.17	0.48	868	260	198	0.91 (0.98)
$(PDMS-PS-PDMS)_l$ 19/36/19	18 600–35 800–18 600	1.15	0.48	868	260	218	0.91 (0.98)
$(PS-P2VP)_c$ 39/38	38 700–38 700	1.36	0.50	565	72	202	0.91 (0.95)
$(P2VP-PS-P2VP)_l$ 19/39/19	19 350–38 700–19 350	1.31	0.50	565	72	221	0.91 (0.95)

[a] Determined by SEC. [b] Determined by ^{1}H NMR. [c] Determined by SAXS, ±2 Å. [d] ±0.02, theoretical values in parentheses.

vertex functions are derived from the intersegment correlation functions describing the system. After applying the conditions for an extremum in Ω and Fourier transforming, $\Omega[\varrho_A(\mathbf{r})]$ becomes

$$\Omega[\varrho_A(\mathbf{k})] = \frac{k_BT}{2\varrho V}\sum_{\mathbf{k}\neq 0}\Gamma_2(\mathbf{k},-\mathbf{k})\,\varrho_A(\mathbf{k})\,\varrho_A(-\mathbf{k}) + \frac{k_BT}{6\varrho^2V^2}\sum_{\mathbf{k}_1,\mathbf{k}_2\neq 0}\Gamma_3(\mathbf{k}_1,\mathbf{k}_2,-\mathbf{k}_1-\mathbf{k}_2)\,\varrho_A(\mathbf{k}_1)\,\varrho_A(\mathbf{k}_2)\,\varrho_A(-\mathbf{k}_1-\mathbf{k}_2) + \frac{k_BT}{24\varrho^3V^3}\sum_{\mathbf{k}_1,\mathbf{k}_2,\mathbf{k}_3\neq 0}\Gamma_4(\mathbf{k}_1,\mathbf{k}_2,\mathbf{k}_3,-\mathbf{k}_1-\mathbf{k}_2-\mathbf{k}_3)\times \varrho_A(\mathbf{k}_1)\,\varrho_A(\mathbf{k}_2)\,\varrho_A(\mathbf{k}_3)\,\varrho_A(-\mathbf{k}_1-\mathbf{k}_2-\mathbf{k}_3) + \ldots \quad (1)$$

where k_BT and V are Boltzmann's constant multiplied by absolute temperature and the total system volume, respectively. Ω is calculated by summing over the contributions of all $\mathbf{k}$, thereby accounting for all modes comprising the density profile in the ordered state. Moreover, the summation over all $\mathbf{k}$ captures the internal excitations of the polymer chains and is crucial to the application of this formalism to systems in the intermediate- and strong-segregation regimes.[20] In the present calculation, we will truncate eq 1 to the term containing Γ_2, since predictions for diblock copolymers in the intermediate- and strong-segregation regimes indicate that this truncation is a reasonable approximation to the full expression.[18]

In general, the vertex functions Γ_i are calculated within the random-phase approximation (RPA)[21] and are dependent upon the block copolymer architecture, composition, f, and degree of quench into the microphase-separated state, χN. We are concerned with comparing the properties of cyclic diblocks with their linear diblock and of precursor linear triblock analogues. Therefore, in our calculation, we employ expressions for Γ_2 for A–B linear diblocks,[21] A–B–A linear triblocks,[22] and cyclic A–B diblocks.[24]

To reduce the computational effort, we utilize the technique of density profile parametrization[17,18] to describe $\varrho_A(\mathbf{k})$ for the lamellar microstructures we will consider. The expressions for Γ_2 and the parametrized forms of the density profiles introduce D/R_g and σ_0/D as the variational parameters in our theory. By specifying values of f and χN, minimizing Ω with respect to these parameters yields the periodicity of the ordered microstructure, D, and the width of the interface separating the A-rich and B-rich microdomains, σ_0. To facilitate a comparison of the properties of the cyclic systems with their linear analogues, we choose the radius of gyration, R_g, to be that of a linear, Gaussian chain having N statistical segments of length a ($R_g = (N/6)^{1/2}a$).

In our development we have ignored the contributions of the higher-order vertex functions to the free energy. These terms are necessary to adequately address systems in the weak-segregation regime near the microphase-separation transition (MST), that is, for $\chi N \sim (\chi N)_{MST}$. However, the present form of Ω is successful in describing systems when $\chi N \gg (\chi N)_S$, where $(\chi N)_S$ is χN at the spinodal. This was demonstrated for lamellae-forming linear A–B diblock copolymer systems by comparing the behavior of D and σ_0 as a function of χN using the first three terms of eq 1 (with Γ_3 and Γ_4 evaluated in the local approximation[23]) with that observed when only the first term of eq 1 is retained.[18] With either expression, a well-defined crossover between the intermediate- and strong-segregation regimes is observed in the scaling of D with χN at $\chi N \sim 100$. Further, in these regimes the behavior of D and σ_0 as a function of χN is virtually identical in both cases. Each form recovers the established results, $D \sim \chi^{1/6}N^{2/3}$ and $\sigma_0 \sim \chi^{-1/2}$ in the strong-segregation regime.[23,25,26]

We have also ignored any effects arising from composition fluctuations in the homogeneous phase.[27] This is justified in our case since our focus is on systems in the intermediate- and strong-segregation regimes. A recent calculation for A–B diblock copolymers finds that any effects due to composition fluctuations in the homogeneous phase die rapidly for systems quenched below the MST, with mean-field behavior recovered when $\chi N > (\chi N)^*_{MST} + 1$, where $(\chi N)^*_{MST}$ is the calculated value of χN at the microphase-separation transition including the effect of composition fluctuations in the homogeneous phase.[20]

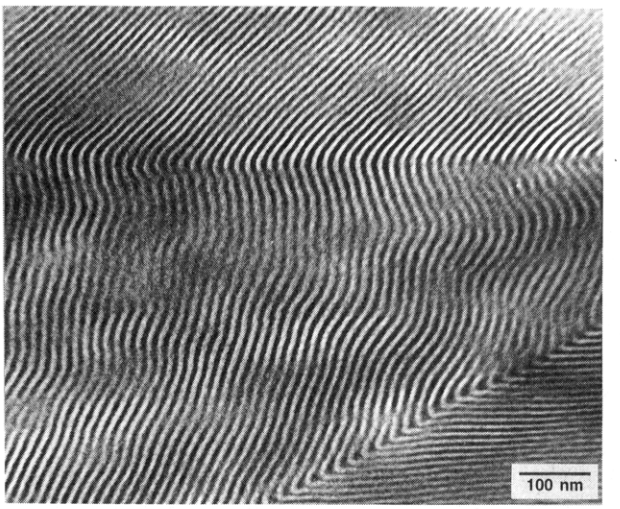

Figure 1. Bright-field TEM micrograph of $(PS-PDMS)_c$ 15/12. The PDMS domains appear dark in the micrograph. Note the presence of "chevron" and "omega" tilt grain boundaries in this well-ordered, lamellae-forming system.

Figure 1 is a bright-field TEM micrograph of unstained $(PS-PDMS)_c$ 6/15/6. In this figure, the dark and light regions correspond to the PDMS and PS components, respectively. Figure 1 is typical of the six systems studied here, since all systems are nearly symmetric in composition and display well-ordered lamellar microdomains. Note that "chevron" and "omega"

tilt grain boundaries are also observed in this image and serve as an additional characteristic signature of lamellar ordering.[28] The domain spacing, D, of each sample was precisely determined by SAXS to an accuracy of ±2 Å by integrating the (001) diffraction ring exhibited by each sample. Additional orders of diffraction were quite weak, with near extinction of even orders expected for all samples since $f \simeq 0.5$. These results are shown in Table 1. The most interesting feature of this data is that, for a given cyclic diblock/linear triblock pair, the cyclic species *always* has a smaller domain spacing. This ~5−10% difference is physically significant for the theoretical reasons presented below.

In order to understand the origin of the observed dependence of D on architecture, we consider the ratio of the domain spacing of the cyclic diblock to its linear analogue, D_c/D_l. For the cyclic diblock/linear triblock pairs, we find that $D_c/D_l = 0.95$ for $(PS-PDMS)_c$ 15/12 and $(PDMS-PS-PDMS)_l$ 6/15/6, 0.91 for $(PS-PDMS)_c$ 36/38 and $(PDMS-PS-PDMS)_l$ 19/36/19, and 0.91 for $(PS-P2VP)_c$ 39/38 and $(P2VP-PS-P2VP)_l$ 19/39/19. For these systems, the error in the experimental D_c/D_l is ±0.02. It is useful to express the data in this fashion for the following reasons. Since the molecular weight, composition, and sample preparation conditions are identical for each pair, they are at the same degree of quench. Therefore, χN and f are *identical* for a given pair. Also, since $(\chi N)_S$ is nearly equal for each triblock and ring system (to be discussed below), each pair is at virtually the same *degree* of segregation. Therefore, the D_c/D_l ratio should only reflect differences in the *topology* of the molecules. Finally, analyzing the experimental data in this fashion facilitates a comparison with the theoretical predictions by eliminating the need to experimentally determine R_g for each system.

To enable a comparison of the set of experimental D_c/D_l to those predicted by our calculation to be discussed below, we evaluate χN at the sample preparation conditions. N is calculated based on the pure-component densities and composition of each system, assuming narrow interfaces and a negligible volume change upon mixing,[25] and is given for each system in Table 1. For the PS−PDMS systems, we estimate $\chi_{PS-PDMS} \simeq 0.3$ at our sample preparation conditions.[30] Then for $(PS-PDMS)_c$ 15/12 and $(PDMS-PS-PDMS)_l$ 6/15/6, $\chi N = 89$, and for $(PS-PDMS)_c$ 36/38 and $(PDMS-PS-PDMS)_l$ 19/36/19, $\chi N = 260$. For PS−P2VP systems, $\chi_{PS-P2VP}(T) = 63/T\,(K) - 0.033$.[29] Evaluating $\chi_{PS-P2VP}$ at 115 °C, we estimate, for $(PS-P2VP)_c$ 39/38 and $(P2VP-PS-P2VP)_l$ 19/39/19, $\chi N = 72$.

Part a of Figure 2 is a double-logarithmic plot of D/R_g versus χN for symmetric ($f = 0.5$) A−B cyclic diblocks, A−B linear diblocks, and A−B−A linear triblocks. We find that the strong-segregation regime begins at $\chi N \sim 100$ for each system, based on the observed scaling behavior $D \sim N^{2/3}$ when $\chi N \geq 100$. We also observe this result when $f = 0.4$ and $f = 0.6$ for these systems when $\chi N \geq 100$. Further, for each of the architectures considered, D/R_g varies by less than 1% over $f = 0.40-0.60$ at a particular value of χN. Therefore, we expect that the calculated behavior for symmetric systems should be well applicable to the experimental systems considered here despite their slight compositional asymmetry. Previously we stated that the present calculation should be valid for $\chi N \gg (\chi N)_S$, that is, for the intermediate- and strong-segregation regimes. In order to estimate the onset of the intermediate-segregation regime for the cyclic diblock and linear triblock systems,

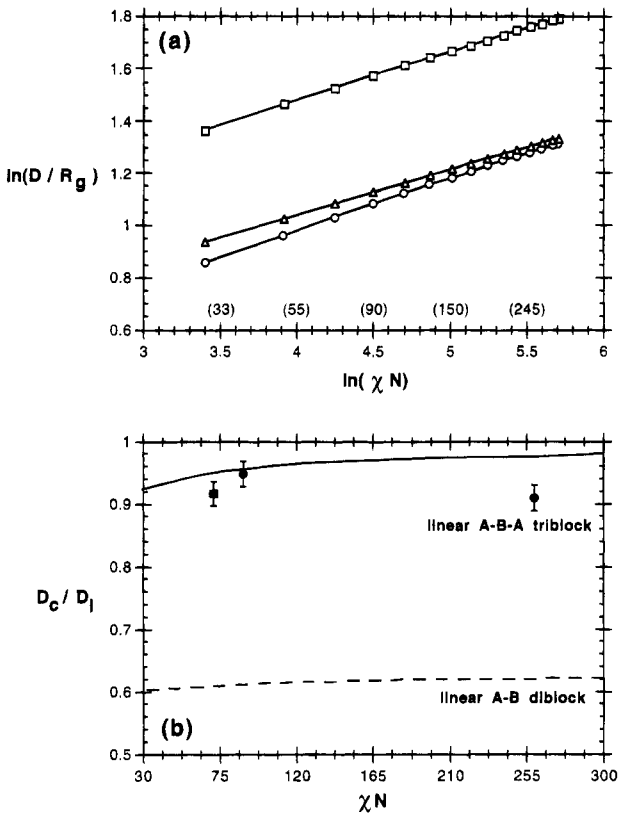

Figure 2. (a) Double-logarithmic plot of D/R_g versus χN for symmetric A−B cyclic diblock (○), A−B−A linear triblock (△), and A−B diblock (□) copolymers as predicted by density functional theory. The values of χN are given above the abscissa for selected values of $\ln(\chi N)$. A transition from $D \sim N^{0.72}$ to $D \sim N^{2/3}$ is observed at $\chi N \sim 100$, indicating the expected onset of strong-segregation behavior when $\chi N \geq 100$. (b) Plot of D_c/D_l versus χN from the data shown in part a and for the PS/PDMS (●) and PS/P2VP (■) systems.

we find from part a of Figure 2 that $D \sim N^{0.72}$ for these systems when $\sim 30 < \chi N < 100$. For symmetric, lamellae-forming A−B diblocks, the onset of the intermediate-segregation regime occurs at about $\chi N = 12.5$ and exhibits similar scaling behavior until the crossover to strong-segregation behavior occurs at $\chi N \sim 100$.[17] Since $(\chi N)_{MST} \sim (\chi N)_S = 17.995$[22] and $(\chi N)_{MST} = (\chi N)_S = 17.795$[24] for symmetric A−B−A triblock and A−B cyclic diblock systems, respectively, we propose that $\chi N = 30$ is a conservative estimate for the onset of the intermediate-segregation regime for these systems. In light of these arguments, we conclude that the experimental systems span the intermediate- and strong-segregation regimes based on their respective values of χN. This observation justifies, in part, the use of the truncated version of the theory.

Part b of Figure 2 is a plot of the predicted D_c/D_l versus χN for symmetric systems derived from part a. The values for the experimentally observed D_c/D_l are also included on this plot. We observe that the predicted values of D_c/D_l are *weakly* dependent on χN. Therefore, other than classifying their degree of segregation, determining the precise value of χN for the experimental systems is not essential when attempting a comparison of the experimental values of D_c/D_l to those predicted by our theory. Over the range $\chi N = 30-300$, $D_c/D_l = 0.60-0.62$ when the linear species is an A−B diblock copolymer and $D_c/D_l = 0.92-0.98$ when the linear system is an A−B−A triblock copolymer.

These results are physically motivated by considering that symmetric A−B cyclic diblocks having N segments

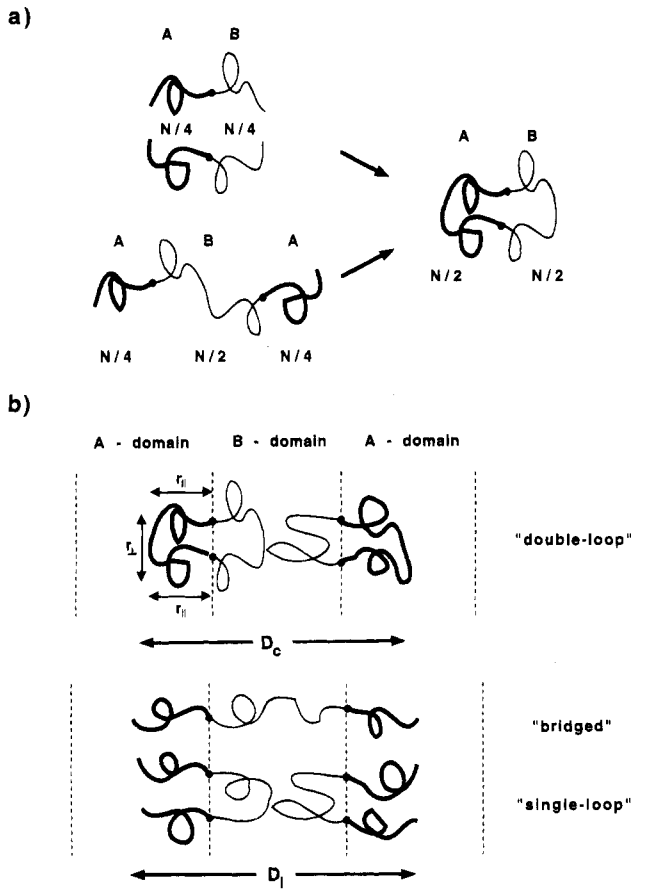

Figure 3. (a) Schematic showing the formation of a symmetric A–B cyclic diblock copolymer composed of N segments from two symmetric A–B linear diblock copolymers each having $N/2$ segments and also from a symmetric A–B–A linear triblock having N segments. (b) Two possible conformations of an A–B–A triblock copolymer in the microphase-separated state characterized by a lamellar long-period D_l: bridged and single loop. The double-looped structure of an A–B cyclic diblock copolymer is shown above. $r_{\parallel} \simeq D_c/2$. The segments composing the loops having trajectories perpendicular to the lamellar normal contribute to $r_{\perp}$ and not to D_c.

can be formed by joining the A and B ends of *two* symmetric linear A–B diblocks having $N/2$ segments or by joining the two A ends of *one* symmetric linear A–B–A triblock copolymer having N segments. This is shown schematically in part a of Figure 3. As shown in part b of Figure 3, the cyclic diblock systems possess doubly-looped chain conformations in the microphase-separated state, and the A–B–A triblock systems are comprised of chains with either bridged or single-loop conformations. The A–B linear diblock systems have no loops.

These characteristics were employed in a recent calculation for symmetric, strongly-segregated, lamellae-forming cyclic and linear A–B diblock copolymers.[24] In part of this study focusing on the weak-segregation regime, a scaling *ansatz*[31] considering the entropy reduction associated with deforming a polymer chain balanced by the decrease in enthalpy arising from the formation of interfaces in the microphase-separated state was used to address strongly-segregated systems. For a symmetric cyclic/linear diblock pair having the same N, this analysis predicts $D_c/D_l \rightarrow 2^{-2/3} \simeq 0.64$ as $\chi N \rightarrow \infty$. A similar scaling analysis indicates $D_c/D_l = 1$ as $\chi N \rightarrow \infty$ for symmetric, lamellae-forming cyclic diblock/linear triblock copolymer pairs. These limiting predictions are recovered by our calculation for $\chi N \gg 300$.

The assumption driving the scaling analyses is that a negligible fraction of the segments in the cyclic diblock and linear triblock copolymers from the loops and do not contribute significantly to $r_{\perp}$, shown in part b of Figure 3. This is expected for deeply quenched systems ($\chi N \rightarrow \infty$) where the chains are exceedingly stretched. However, for finite values of χN, the chains are less stretched than in the limiting case, and a nonnegligible fraction of the chain segments assume trajectories that lie parallel to the lamellar interfaces. This leads to an increase in $r_{\perp}$ and a decrease in D_c. This is also the case for the middle block in the linear A–B–A triblock copolymers assuming looped conformations, which have been predicted to be formed by approximately 60% of the symmetric A–B–A triblock molecules over a wide range of χ and N.[32] Therefore, since the microdomains formed by the triblock copolymers are composed of a mixture of looped and bridged chains, D_l should always be larger than D_c (at finite χN) since the cyclic systems always have more loops per chain. We argue this is the origin of the decreased values of D_c/D_l in the experimental data and the present calculation from that predicted by the scaling analysis.

In summary, we have characterized microphase-separated lamellae-forming, cyclic PS–PDMS and PS–P2VP diblock copolymers as well as their linear triblock precursors. We have directly observed the effect of looped versus bridged chain conformations in the microphase-separated state through an analysis of the relative domain spacings of the lamellae formed by the cyclic diblock and linear triblock systems, with $D_c/D_l < 1$ for all of the systems investigated. This observation is attributed to the differences in architecture between the two systems. The presence of double loops in the A–B cyclic systems versus a mixture of single-loop and bridged conformations in the A–B–A triblock systems is argued to account for the observed behavior. Since each system is at a finite degree of quench, a nonnegligible fraction of segments in the looped portions of the chains assume trajectories which lie parallel to the A–B interfaces and do not contribute to D.

Acknowledgment. We acknowledge support for this work from NSF Grants DMR 92-14853, DMR-9223966, and DMR 91-101558, DoE Grant DE-FG02-87ER60522, and AFOSR Grant F49620-94-1-0224.

References and Notes

(1) Merkle, G.; Burchard, W.; Lutz, P.; Freed, K. F.; Gao, J. *Macromolecules* **1993**, *26*, 2736.
(2) Higgins, J. S.; Dodgson, K.; Semlyen, J. A. *Polymer* **1979**, *20*, 553.
(3) Santore, M. M.; Han, C. C.; McKenna, G. B. *Macromolecules* **1992**, *25*, 3416.
(4) Klein, J. *Macromolecules* **1986**, *19*, 105.
(5) Tead, S. F.; Kramer, E. J.; Hadziioannou, G.; Antonietti, M.; Stillescu, H.; Lutz, P.; Strazielle, C. *Macromolecules* **1992**, *25*, 3942.
(6) Michels, J. P. J.; Wiegel, F. W. *Proc. R. Soc. London, Ser. A* **1986**, *403*, 269.
(7) de Gennes, P.-G. *C. R. Acad. Sci. Paris* **1990**, *310*, 1327.
(8) Koniaris, K.; Muthukumar, M. *Phys. Rev. Lett.* **1991**, *66*, 2211.
(9) Stepto, R. F. T. *Eur. Polym. J.* **1993**, *29*, 415.
(10) Hogen-Esch, T. E.; Sundararajan, J.; Toreki, W. *Makromol. Chem., Macromol. Symp.* **1991**, *47*, 23.
(11) Yin, R.; Hogen-Esch, T. E. *Macromolecules* **1993**, *26*, 6952.
(12) Yin, R.; Amis, E. J.; Hogen-Esch, T. E. *Makromol. Chem., Macromol. Symp.* **1994**, *85*, 217.
(13) Gan, Y. D.; Zoeller, J.; Hogen-Esch, T. E. *Polym. Prepr. (Am. Chem. Soc., Div. Polym. Chem.)* **1993**, *34* (1), 69.

(14) Brandrup, J., Immergut, E. H., Eds. *Polymer Handbook*; Interscience: New York, 1966. $\delta_{toluene} = 8.9$ (cal/cm^3)$^{1/2}$, $\delta_{PS} = 9.1$ (cal/cm^3)$^{1/2}$, $\delta_{P2VP} = 10.0$ (cal/cm^3)$^{1/2}$, and $\delta_{PDMS} = 8.5$ (cal/cm^3)$^{1/2}$.
(15) Thomas, E. L.; Lescanec, R. L. *Philos. Trans. R. Soc. London, Ser. A* **1994**, *348*, 149.
(16) Tate, M. W.; Eikenberry, E. F.; Gruner, S. M., in preparation.
(17) Melenkevitz, J.; Muthukumar, M. *Macromolecules* **1991**, *24*, 4199.
(18) Lescanec, R. L.; Muthukumar, M. *Macromolecules* **1993**, *26*, 3908.
(19) Landau, J. D.; Lifshitz, E. M. *Statistical Physics*; Pergamon Press: Oxford, U.K., 1980; Part 1.
(20) Muthukumar, M. *Macromolecules* **1993**, *26*, 5259.
(21) Leibler, L. *Macromolecules* **1980**, *13*, 1602.
(22) Mayes, A. M.; Olvera de la Cruz, M. *J. Chem. Phys.* **1989**, *91*, 7228.
(23) Ohta, T.; Kawasaki, K. *Macromolecules* **1986**, *19*, 2621.
(24) Marko, J. F. *Macromolecules* **1993**, *26*, 1442.
(25) Helfand, E.; Wasserman, Z. R. *Developments in Block Copolymers*; Goodman, I., Ed.; Elsevier: New York, 1982; Vol. 1.
(26) Vavasour, J. D.; Whitmore, M. D. *Macromolecules* **1992**, *25*, 5477.
(27) Fredrickson, G. H.; Helfand, E. *J. Chem. Phys.* **1987**, *87*, 6.
(28) Gido, S. P.; Thomas, E. L. *Macromolecules* **1994**, *27*, 6137.
(29) Dai, K. H.; Kramer, E. J. *Polymer* **1994**, *35*, 157.
(30) Galin, M.; Rupprecht, M. C. *Macromolecules* **1979**, *12*, 506. χ was determined using gas chromatography of a series of PS–PDMS diblocks and PDMS–PS–PDMS triblock copolymers in a variety of solvents at different temperatures. For our study, we take χ to be that of a lamellar-forming system with toluene as the probe solvent at 120 °C.
(31) Semenov, A. N. *Zh. Eksp. Teor. Fiz.* **1985**, *88*, 1242.
(32) Matsen, M. W.; Schick, M. *Macromolecules* **1994**, *27*, 187.

MA9461198